

---

EFDA–JET–CP(04)07-20

W. Suttrop, V. Hynönen, T. Kurki-Suonio, P.T. Lang, M. Maraschek, R. Neu,  
A. Stäbler, G.D. Conway, S. Hacquin, M. Kempenaars, P.J. Lomas,  
M.F.F. Nave, R.A. Pitts, K-D. Zastrow, the ASDEX Upgrade team  
and JET EFDA Contributors

# Studies of the “Quiescent H-Mode” Regime in ASDEX Upgrade and JET



# Studies of the “Quiescent H-Mode” Regime in ASDEX Upgrade and JET

W. Suttrop<sup>1</sup>, V. Hynönen<sup>2</sup>, T. Kurki-Suonio<sup>2</sup>, P.T. Lang<sup>1</sup>, M. Maraschek<sup>1</sup>, R. Neu<sup>1</sup>,  
A. Stäbler<sup>1</sup>, G.D. Conway<sup>1</sup>, S. Hacquin<sup>3</sup>, M. Kempenaars<sup>4</sup>, P.J. Lomas<sup>5</sup>,  
M.F.F. Nave<sup>3</sup>, R.A. Pitts<sup>4</sup>, K-D. Zastrow<sup>5</sup>, the ASDEX Upgrade team  
and JET EFDA Contributors\*

<sup>1</sup>Max-Planck-Institut für Plasmaphysik, EURATOM Association, D-85748 Garching;

<sup>2</sup>EURATOM-TEKES Association, Helsinki University of Technology, P.O. Box 2200, FIN-02015 HUT, Finland

<sup>3</sup>Associação EURATOM/IST, Centro de Fusão Nuclear, Instituto Superior  
Técnico, 1049-001 Lisboa, Portugal

<sup>4</sup>FOM-Instituut for Plasmaphysica “Rijnhuizen”, Association EURATOM-FOM, P.O. Box 1207,  
3430 Nieuwegein, The Netherlands;

<sup>5</sup>EURATOM/UKAEA Fusion Association, Culham Science Centre, Abingdon Oxon OX14 3DB, UK

<sup>6</sup>Association EURATOM-CRPP, Ecole Polytechnique Fédérale de Lausanne, 1015 Ecublens, Switzerland

\* See annex of J. Pamela et al, “Overview of JET Results”,  
(Proc.20<sup>th</sup> IAEA Fusion Energy Conference, Vilamoura, Portugal (2004)).

Preprint of Paper to be submitted for publication in Proceedings of the  
20th IAEA Conference,  
(Vilamoura, Portugal 1-6 November 2004)

“This document is intended for publication in the open literature. It is made available on the understanding that it may not be further circulated and extracts or references may not be published prior to publication of the original when applicable, or without the consent of the Publications Officer, EFDA, Culham Science Centre, Abingdon, Oxon, OX14 3DB, UK.”

“Enquiries about Copyright and reproduction should be addressed to the Publications Officer, EFDA, Culham Science Centre, Abingdon, Oxon, OX14 3DB, UK.”

## **ABSTRACT.**

The stationary ELM-free “Quiescent H-mode” (QH-mode) regime, obtained with counter neutral beam injection, is studied in ASDEX Upgrade (AUG) and JET. QH-mode plasmas have high pedestal and core ion temperatures together with good H-mode confinement. ELMs are replaced by continuous MHD oscillations, the “Edge Harmonic Oscillation” (EHO) and the “High Frequency Oscillation”. Stationarity of particle and impurity densities is linked to the occurrence of these MHD modes. The EHO location in the steep-gradient region and its appearance with increasing edge pressure points at the edge pressure or pressure gradient as possible drivers for the EHO. Injection of small cryogenic pellets can raise the plasma density somewhat without triggering ELMs. Orbit-following calculations of the slowing down distribution show the presence of an enhanced fast particle density in the H-mode barrier region despite the large loss currents with counter-injection.

## **1. INTRODUCTION**

The “High-confinement” mode (H-mode) is considered a reliable regime for achieving adequate fusion yield in the planned ITER experiment and in a nuclear fusion reactor. However, at the large temperature and pressure values on top of the edge transport barrier (the H-mode “pedestal”), type I Edge Localised Modes (“ELMs”) are usually obtained, which may impose unacceptable peak heat loads on the divertor target in a large scale fusion device, if the ablation thresholds for both metal and graphite divertors are exceeded [1]. Therefore, confinement regimes that allow for large pedestal pressure in order to maintain good confinement, but with small or no ELMs are needed to prevent excessive erosion and migration of divertor material inside the tokamak vessel.

Usually, particle transport across the H-mode barrier occurs mainly during ELMs, so that ELM-free H-modes are typically characterised by accumulation of density and impurities, terminated by a large ELM or thermal collapse. The “Quiescent” H-mode (QH-mode) regime, recently discovered in DIII-D [2] is ELM-free, but with stationary density and impurity content. At the same time, the confinement is comparable to or better than in a typical type-I ELMy H-mode. The QH-mode regime has been reproduced and studied in ASDEX Upgrade [3]. Meanwhile, H-mode behaviour similar to that of a QH-mode has been found in JT-60U [4].

Here we report further studies of QH-mode properties in ASDEX Upgrade (AUG) and experiments to scale up the QH-mode regime to larger plasmas in the Joint European Torus (JET). The next two sections summarise the conditions and phenomenology of the QH-mode in both machines. Subsequently, we describe the properties of the MHD behaviour that replaces ELMs in QH-mode and discuss the possible reasons for the suppression of ELMs in this regime.

## **2. PHENOMENOLOGY OF QH-MODE IN ASDEX UPGRADE**

So far in ASDEX Upgrade, QH-mode has been only seen with counter-current Neutral Beam Injection (counter-NBI). In agreement with experience in DIII-D [2], large plasma-wall clearance (in AUG

typically 8cm gap in the main chamber), good pumping (using the lower divertor cryopump), and low neutral gas pressure appear helpful in obtaining long stationary QH-mode phases. The experiments have been carried out with a plasma current of  $I_p = 1\text{MA}$  and a toroidal field  $B_t$  between 2.0 and 2.5T ( $q_{95} = 3.6\dots 4.5$ )

Figure 1 shows time traces of two pulses that enter QH-mode: Pulse No: 17686 with a mixture of 2 semi-tangential NBI sources (one at  $E = 60\text{keV}$  beam energy with tangency radius  $R_{\text{tan}} = 0.93\text{m}$  and one at  $E = 93\text{keV}$  with  $R_{\text{tan}} = 0.84\text{m}$ ), and Pulse No: 17694 with two radial sources ( $E = 60\text{keV}$  with  $R_{\text{tan}} = 0.53\text{m}$ ). The plasma configuration and total NBI heating power are identical. The transition to QH-mode occurs earlier and the QH-mode phases are longer with more tangential injection, in line with observations at DIII-D [5]. Note that with more tangential injection the plasma density remains constant or drops after the transition to QH-mode, while with radial injection both edge and core densities, after an initial drop, increase to levels above those in ELMy H-mode before the transition. A transition to QH-mode is also obtained with the pair of tangential NBI sources installed at AUG ( $E = 93\text{keV}$  with  $R_{\text{tan}} = 1.29\text{m}$ , on the high field side), but the density quickly drops below the minimum density to avoid NBI shine-through. Note that while radial and semi-tangential sources produce trapped particles in a wide radial range, the tangential sources produce mostly passing particles inside the plasma, and a significant trapped particle fraction only near the H-mode pedestal. In AUG, QH-mode has been obtained at various levels of effective ion charge  $Z_{\text{eff}}$ , the lowest value obtained so far being  $Z_{\text{eff}} = 2.5$  [6]. ELMy and QH-mode phases with counter injection show similar values of  $Z_{\text{eff}}$ .

### 3. QH-MODE EXPERIMENTS IN JET

During the 2003 reversed plasma current campaign in JET, dedicated experiments were carried out to identify the QH-mode regime in plasmas of larger size. The configuration used (shown in the insert in Fig.2) combines large wall clearance (15cm outboard and inboard gaps) and good exhaust by positioning the strike points for optimum cryo-pumping in the Mark II SRP Gasbox divertor. Low recycling conditions are obtained by a combination of He glow discharge cleaning followed by a lengthy period of cryo-pumping and beryllium evaporation in the main chamber. Discharges are heated with up to 14MW of counter current neutral beams. Different combinations of plasma current and magnetic field are used: 2.5MA/ 2/7T ( $q_{95} = 3.3$ ), 1.7MA/2.15 T ( $q_{95} = 4.9$ ), 1.7MA/ 2.25T ( $q_{95} = 4.3$ ) and 1.5MA/2.2 T ( $q_{95} = 4.7$ ).

In these discharges, extended ELM-free phases with up to 1.5s duration are found. Figure 2 (a) shows Pulse No: 59611 ( $I_p = 2.5\text{MA}$ ,  $B_t = 2.7\text{T}$ ,  $q_{95} = 3.3$ ) with type I ELMs until  $t = 17.2\text{s}$ , followed by an ELM-free phase until 18.6s. During the ELM-free time interval, radiated power (top panel) and electron density (third panel) remain stationary, indicating that the particle confinement time is not drastically increasing in the absence of ELMs. This behaviour is as expected for QH-mode and in contrast to the density and radiation rise usually found in traditional ELM-free phases.  $Z_{\text{eff}}$  is high, as is often seen in the smaller machines with counter-injection at low density, ranging between 4 and 5 in

JET, independent of the presence of ELMs. Confinement is at or above the H98y scaling, and no deterioration during the ELM-free phase is seen. These stationary ELM-free phases are accompanied by the characteristic Edge Harmonic Oscillation (EHO), which is observed both in magnetic measurements and in X-mode reflectometry measurements with cut-off layer in the H-mode barrier region. Therefore we identify these phases as transitions to the QH-mode regime in JET. In addition, pronounced core MHD behaviour is observed in most discharges. While the cases with  $q_{95} = 3.3$  have sawteeth, the plasmas at higher  $q$  ( $q_{95} = 4$ ) generally show  $n = 1, m = 1$  fishbone activity.

In Figure 2 (b), core temperature and density profiles of an ELMy and a QH-mode phase are compared in the same discharge. The ECE and charge exchange spectroscopy measurements (edge and core systems) indicate that there is little difference in electron and ion temperatures through most of the profile and at the H-mode pedestal top. Also, as shown by core LIDAR measurements, the plasma density is similar in the two regimes.

Although the observed ELM-free phases show many of the features characteristic of the QH regime, it has not been possible in JET to reproduce the same behaviour in repetitive pulses with identical parameters or to produce extended QH-mode periods for longer than about 1.5 or three confinement times. It appears that the longest quiescent phases occur in plasmas produced immediately after the wall conditioning cycles or following repeated low recycling discharges with high NBI power and minimum external gas input.

#### **4. MHD ACTIVITY IN QH-MODE**

QH-mode pulses usually show rich MHD activity. In the plasma core, fishbone or continuous  $m = 1, n = 1$  oscillations prevail at higher edge safety factor while at low  $q$  sawtooth oscillations occur. A range of discharges has no discernible  $m = 1, n = 1$  activity.

##### **4.1. THE “EDGE HARMONIC OSCILLATION”.**

The most pronounced MHD feature of the QH mode is that ELMs are replaced by the characteristic “Edge Harmonic Oscillation” (EHO, [2]). The name originates from the many harmonics observed in spectrograms of magnetic measurements. In AUG and JET, the EHO fundamental has so far always been found at a toroidal mode number  $n = 1$ . ECE and radially deconvoluted Soft X-ray measurements in AUG as well as microwave reflectometer data in JET show that the EHO is located in the H-mode edge transport barrier region. A safety factor scan in AUG shows that the poloidal mode number adjusts itself as for the EHO to remain localised on a flux surface in the gradient region [6]. Also, the ECE measurement reveals that the perturbations outside and inside the rational surface are in phase as expected, e.g., for a kink mode, and in contrast to a magnetic island.

Magnetic measurements at different toroidal locations show practically identical waveforms, phase shifted according to the toroidal angle of the measurement as expected for an  $n = 1$  mode. This suggests that the EHO is a rigidly rotating mode, i.e., the harmonic spectrum originates from its spatial structure, not from a time-dependent perturbation in the rotating frame.

Figure 3 shows the EHO waveform as seen by a radial field pick-up coil in AUG (measuring  $dB_r/dt$ ) which is located 10cm from the separatrix at the outer midplane (upper trace). The raw signal is smoothed by a comb filter set to pass the EHO fundamental and its harmonics and reject noise at other frequencies. The filtered signal is integrated, resulting in a signal proportional to  $B_r$  (middle trace). For a kink-like perturbation the radial field  $B_r$  is proportional to the spatial derivative  $d\xi/dl$  along a field line. Thus, for a rotating mode, the time integral of  $B_r$  gives a signal which is proportional to  $\xi$  as a function of toroidal angle. This signal is shown in the bottom trace. The sharp minima and maxima of the raw magnetic signal, which give rise to the pronounced harmonic spectrum of the EHO, correspond to regions of large curvature near the minima and maxima of  $\xi$ . The EHO waveform can be described as near triangular.

#### **4.2. THE “HIGH FREQUENCY OSCILLATION”.**

In addition to the EHO, an MHD oscillation at high frequencies occurs in AUG [3], typically between 300 and 450kHz and with a toroidal mode number of  $n = 5$ . Often, an additional higher frequency signal (not at an integer multiple frequency) is observed. The HFO amplitude is modulated in time (seen as characteristic bursts) as shown in Fig.4 which compares the EHO signal (taken here from a peripheral Soft X-ray chord), a  $B_r$  measurement with 2MHz bandwidth to resolve the HFO, and outer divertor  $D_\alpha$  intensity. The HFO envelope, with a toroidal  $n = 0$  structure, has the same frequency and a fixed phase relationship with the EHO cycles for each toroidal location.

#### **4.3. TRANSPORT ASSOCIATED WITH EDGE MHD ACTIVITY.**

The absence of ELMs in H-mode usually causes a large increase of the particle confinement time, typically leading to an accumulation of deuterium and impurities, often terminated by an unusually large ELM or a thermal collapse of the plasma. In contrast, the density and radiation in QH-mode are quite stationary. One may ask whether the pronounced edge MHD causes or at least contributes to particle and energy loss across the separatrix. Indeed, the HFO bursts and EHO cycles are strongly correlated with the outer divertor  $D_\alpha$  intensity (Fig.4). The inner divertor  $D_\alpha$  signal shows no correlation. The  $D_\alpha$  time lag of about 20 $\mu$ s [3] is consistent with the loss of neutral beam slowing down deuterium ions (with energy of the order of 1keV) to the divertor. If there are losses of thermal particles, they are overwhelmed by this signal.

Indirect evidence of thermal particle and heat losses associated with edge MHD in QH-mode comes from other observations. Figure 5 shows time traces of AUG shot 18931, in which four pellets have been injected into a QH-mode plasma. The first three pellets result in a moderate but clearly visible increase of the core density. After the fourth pellet, the EHO disappears as seen by the drop of the amplitude in the magnetic signal  $\dot{B}_r$ . After this time, the central and peripheral line densities are no longer stationary but continue to rise until several ELMs occur. Hence, the disappearance of the EHO marks the loss of QH-mode and density control.

With counter neutral beam injection, the EHO is often visible in ELM phases as well, as shown



in Fig.6. The ELM times are identified by the spikes in the divertor  $D_\alpha$  signal. During the ELM cycle, the EHO (from measured  $\dot{B}_T$  in between ELMs) appears only shortly before an ELM. The edge line density and pedestal-top electron temperature (second panel) drop due to the particle and energy losses associated with each ELM and recover quickly in about the first half of the inter-ELM cycle, and remain almost saturated for the second half. The product of these signals is indicative of the pedestal top pressure, which shows the same temporal behaviour. The onset of the EHO in each cycle coincides with the beginning of the pressure saturation.

Since the heat flux from the plasma interior is continuous, this temporal behaviour suggests that with the onset of the EHO heat transport across the edge barrier increases. In addition, the disappearance of the EHO after each ELM and its onset at the time the pressure recovers suggests that the pressure or edge pressure gradient in the barrier region plays a role in driving the EHO.

In order to study impurity transport across the H-mode barrier, silicon is injected into a QH mode plasma by laser-blow-off from a solid target (Fig.7). The silicon content in the plasma core is monitored by a crystal Bragg spectrometer that measures the intensity of a Si XIII (He-like) line at a wavelength of 0.665nm. After the short injection pulse at  $t = 2.59$ s, the intensity drops with a time constant of several hundred milliseconds, despite the increasing electron density. This time scale is similar to that determined in Ref. [7] for Si in ELMy H-mode plasmas with co-injection. We conclude that there is measurable impurity transport across the barrier in QH-mode.

#### **4.4. EFFECTS OF FAST PARTICLES.**

In QH-mode, a strong enhancement of the charge exchange neutral particle flux at high particle energies is observed [3]. Since the density of recycling neutrals in QH-mode is at or below that in ELMy H-mode, the enhancement of the charge exchange flux indicates a strong increase of the fast ion population at the plasma edge. The neutral beam slowing-down distribution is simulated using the Monte Carlo based particle following code ASCOT [8]. The magnetic equilibrium as well as the plasma temperature and density profiles are extracted from the ASDEX Upgrade QH-mode Pulse No: 17695 at  $t = 5.6$ s. Two NBI sources ( $E = 60$ keV,  $R_{\text{tan}} = 0.93$ m) produce a flux of  $\Gamma_{\text{NBI}} = 7.3 \times 10^{20}$  particles/second. The ionisation profiles for full, half and third energy components of the beam are calculated by the FAFNER code [9]. From the initial ion distribution (birth position, energy and pitch angle), a set of  $10^5$  test particles is generated, and the slowing down is followed in ASCOT down to twice the thermal velocity. Orbits that intersect the limiter are counted as losses; the radial flux by these loss orbits is recorded as a function of radius. For counter-injection, the region for significant loss current is found to extend into the plasma down to  $\rho_p = 0.7$ . The four-dimensional distribution function is recorded as the total time spent in slots of  $\rho_p$ , poloidal angle, and parallel ( $v_{\parallel}$ ) and perpendicular ( $v_{\perp}$ ) velocities. In a given phase space volume, the total number of actual plasma particles is the total time spent by test particles, multiplied by the ratio of particle source rate to number of test particles. Thus summing over all test particles during the simulation corresponds to steady-state injection. Figure 8 shows contour plots of a section of the fast particle distribution as a function of  $\rho_p$  and  $v_{\perp}$  for Pulse

No: 17695 (a), and for the corresponding co-injection case, obtained by reversing the initial pitch angles in the simulation (b).

For counter injection (Fig.8(a)), the maximum fast particle density extends further outward (to about  $\rho_p = 0.93$ ) than for its co-injection counterpart ( $\rho_p = 85$ , Fig.8(b)). With the given beam geometry, almost all particles ionised near the H-mode pedestal top are trapped. Because of the outward-opening orbits in counter-injection there is a significant number of particles automatically aligned so that their orbits extend into the region of steep gradient and, hence, to the resonant flux surface of the EHO. This population exists despite strong orbit losses from the plasma edge.

Fast particles can interact with modes in different ways, the effect can be stabilising by finite Larmor radius stabilisation or de-stabilising, if a resonance between the particle motion (bounce frequency or toroidal drift precession frequency) occurs. For the magnetic field configuration used in the present counter-injection experiments, in the absence of a radial electrical field the toroidal drift precession is directed opposite to the injection direction, while both the EHO and HFO rotate in the injection direction (electron drift direction). A sufficiently large inward directed radial electrical field can reverse the precession drift. In fact, in a fully established QH-mode, the  $E_r$  well in the H-mode barrier region is significantly larger than in an ELMy H-mode. This is measured, independently, by Doppler reflectometry in ASDEX Upgrade [10] and, using the radial force balance, from charge exchange spectroscopy in DIII-D [5]. Single particle calculations with ASCOT indicate that the radial electrical field profile in QH-mode obtained from Ref. [10] does in fact reverse the precession drift. Hence it is possible that a resonance with the HFO or the EHO can occur. An analog observation of an edge kink mode destabilised by fast particles might be the appearance of the “outer mode” in JET D-T discharges after giant ELM events when the alpha-particle population slowly restores [11].

## SUMMARY AND DISCUSSION

The quiescent H-mode regime combines stationary good confinement, high pedestal pressure, and low pedestal collisionality ( $\nu < 1$ ) with the absence of ELMs. So far, QH-mode is obtained only with counter-neutral beam injection. Good pumping conditions, achieved e.g. by placing the strike points in a position for good divertor pumping, seem to facilitate access to QH-mode. However, it is not yet possible to quantify the access conditions for QH-mode. Longest QH-mode phases in ASDEX Upgrade (ELM-free for the entire heating phase) and JET (ELM-free for about 1.5s) have been found after fresh vessel conditioning, but it is difficult to say whether the change in the recycling conditions or suppression of impurity in flux is influencing QH-mode access. High  $Z_{\text{eff}}$  is often found with counter injection, but it is not necessarily an essential property of QH-mode. The impurity mix in QH-mode and ELMy phases with counter-NBI is quite similar and depends more on the machine conditions than on the presence or absence of ELMs. Edge transport in QH-mode seems to be linked with the occurrence of the Edge Harmonic Oscillation and the High Frequency Oscillation, which are always seen in QH-mode phases, and sometimes also in between ELMs. So far, the EHO is observed only with counter-NBI in ASDEX Upgrade. It is also unclear whether QH-mode discharges can be

fuelled up to densities near the Greenwald limit. Gas puffing usually leads to a rapid transition to ELMy H-mode. First experiments with pellet fuelling show that pellets do not trigger ELMs in a QH-mode as they usually do in ELMy H-modes with co-NBI [12]. So far, the density increase is limited to about 40% of the Greenwald density. The QH-mode density limit is marked by disappearance of the EHO and a transition to a non-stationary phase terminated by ELMs.

A related, interesting question is what causes the suppression of ELMs in QH-mode. The main observations are as follows:

1. The edge current and pedestal top pressure in the barrier are not reduced compared to ELMy H-mode. This is likely to be true of the current density and pressure gradient as well.
2. In fully established QH-mode, the Er well is significantly larger than in ELMy H-mode.
3. With counter-NBI, a significant population of trapped high-energy particles exists in the barrier region.

The first observation implies that reaching the same edge pressure gradient and the same edge current density as just before ELMs is not sufficient to generate an ELM event. The latter two observations point at a possible suppression of ELMs either by strong  $E \times B$  velocity shear or by finite Larmor radius stabilisation by fast particles. These possibilities will have to be further investigated both experimentally and theoretically.

#### **ACKNOWLEDGEMENT:**

The authors would like to thank S. Günter for valuable discussions and CSC, the Finnish IT centre for science, Espoo, Finland ([www.csc.fi](http://www.csc.fi)) for providing the resources to run the ASCOT code.

#### **REFERENCES**

- [1]. Federici, G. et al., *J. Nucl. Mater.* **313-316** (2003) 11.
- [2]. Burrell, K. H. et al., *Plasma Phys. Controlled Fusion* **44** (2002) A253.
- [3]. Suttrop, W. et al., *Plasma Phys. Controlled Fusion* **45** (2003) 1399.
- [4]. Sakamoto, Y. et al., *Plasma Phys. Controlled Fusion* **46** (2004) 299.
- [5]. Burrell, K. H. et al., *Plasma Phys. Controlled Fusion* **46** (2004) 165.
- [6]. Suttrop, W. et al., *Plasma Phys. Controlled Fusion* **46** (2004) A151.
- [7]. Dux, R. et al., *Plasma Phys. Controlled Fusion* **45** (2003) 1815.
- [8]. Heikkinen, J. A. et al., *Plasma Phys.* **4** (1997) 3655.
- [9]. Lister, G. G., A fully 3-d neutral beam injection code using monte carlo methods, Technical Report 4/222, IPP, Garching, Germany, 1985.
- [10]. Conway, G. D. et al., *Plasma Phys. Controlled Fusion* **46** (2004) 951.
- [11]. Cottrell, G. A. et al., *Nucl. Fusion* **33** (1993) 1365.
- [12]. Lang, P. T. et al., *Nucl. Fusion* **44** (2004) 665.

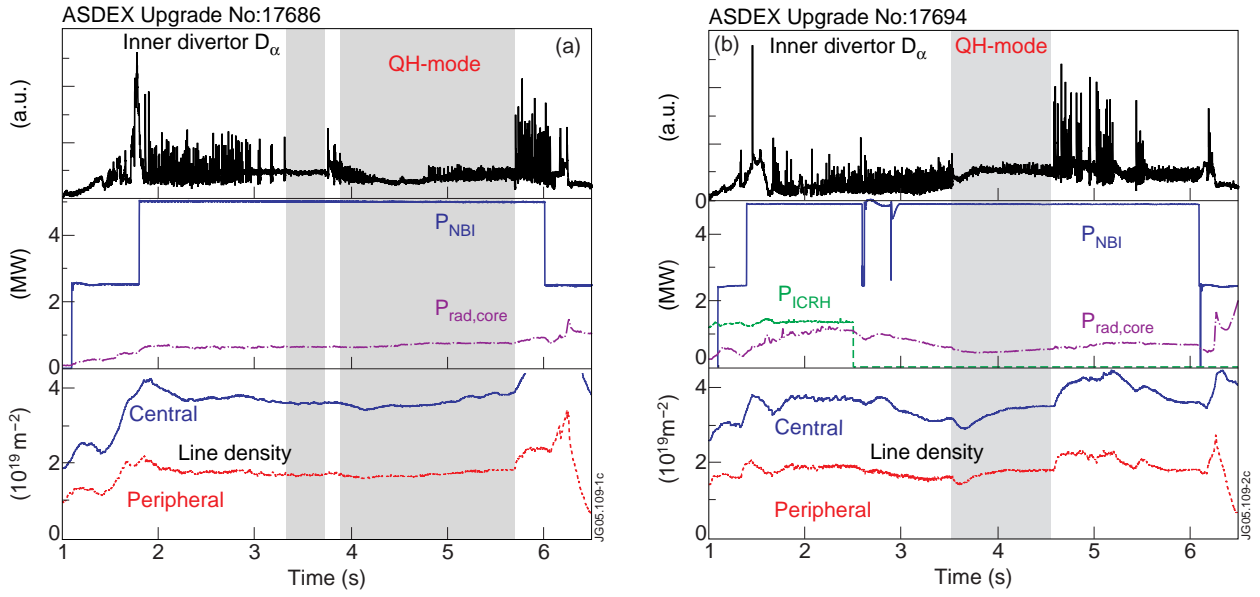


Figure 1: QH-mode in AUG with (a) semi-tangential and (b) radial NBI sources.

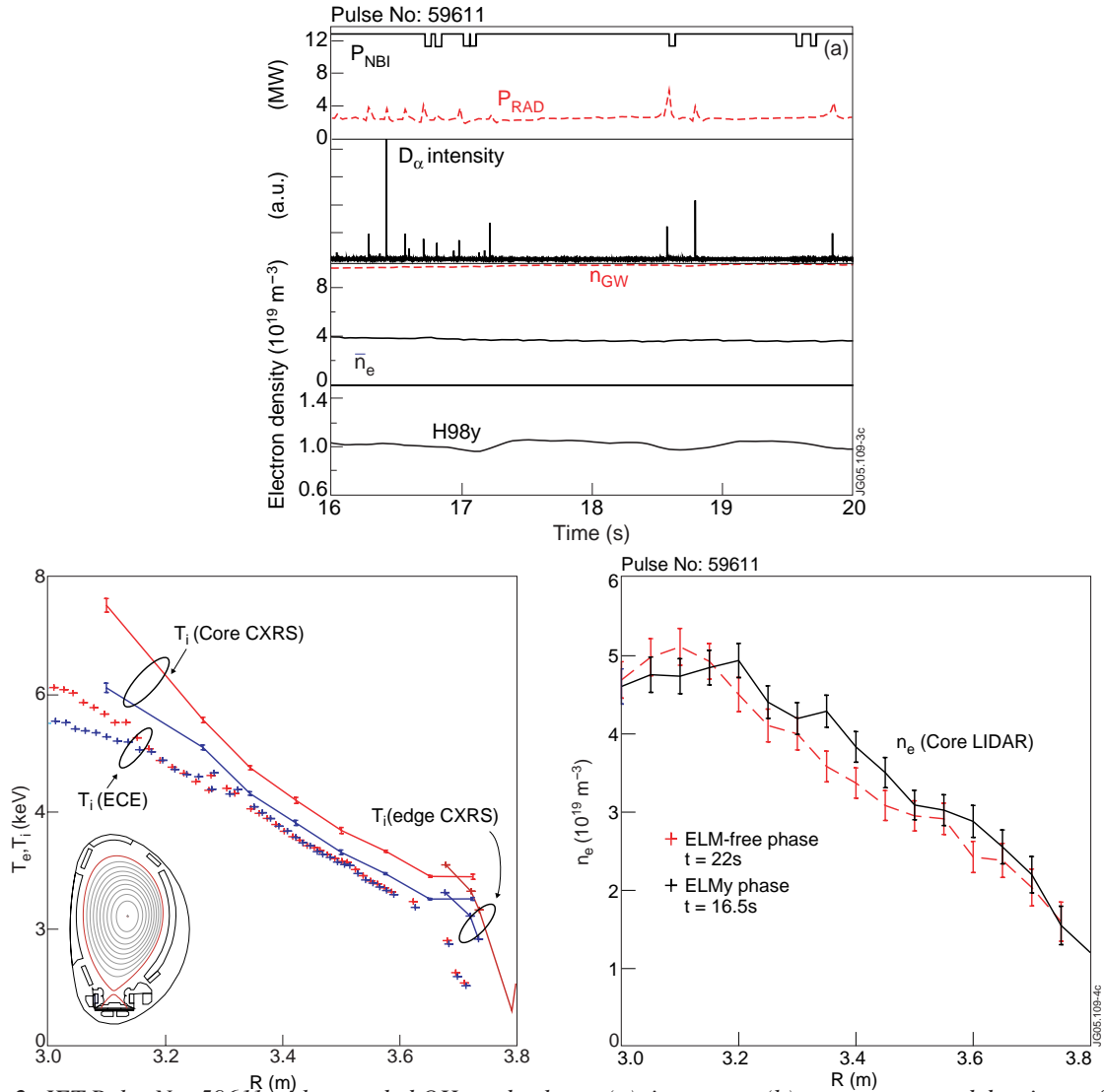


Figure 2: JET Pulse No: 59611 with extended QH-mode phase: (a) time traces (b) temperature and density profiles in ELMy and QH phases.

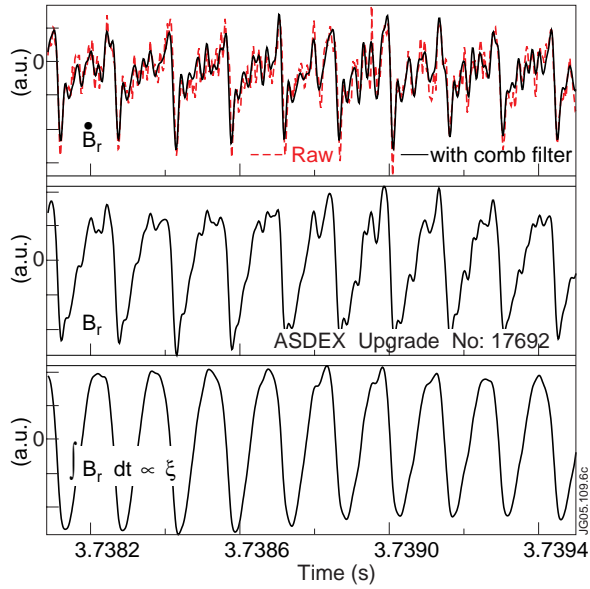


Figure 3: EHO signal as measured by a magnetic probe (top), integrated once for  $B_r$  (middle) and integrated twice, yielding a signal proportional to the radial displacement  $\xi$  (bottom).

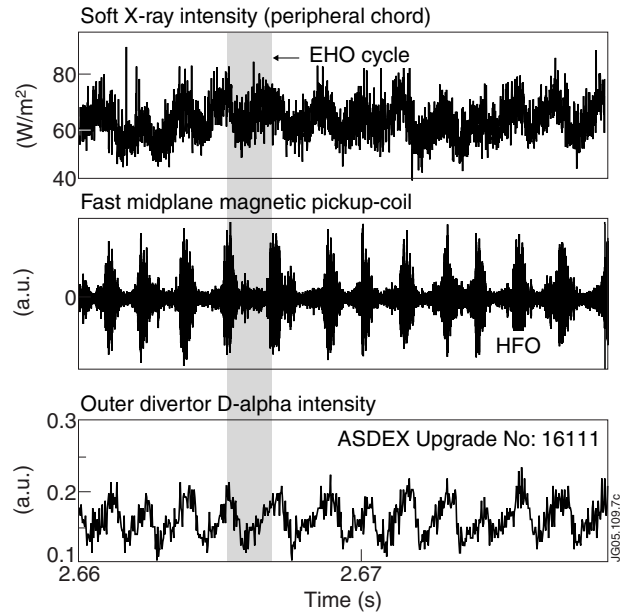


Figure 4: “High Frequency Oscillation” (HFO) and the temporal relation of HFO bursts with EHO cycles.

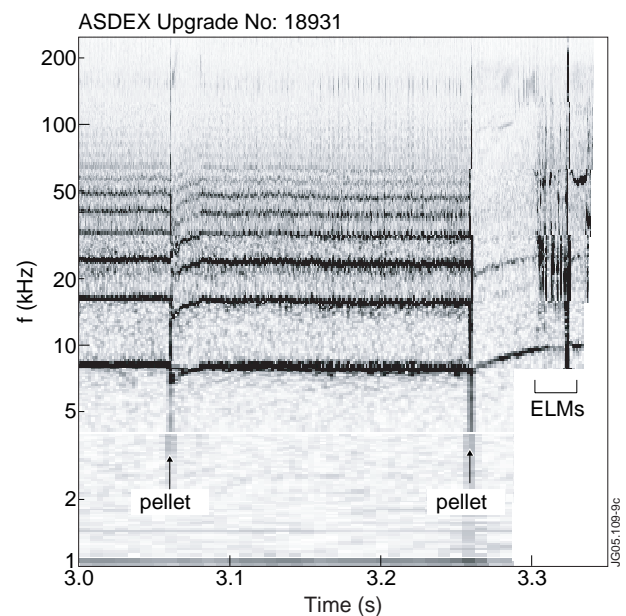
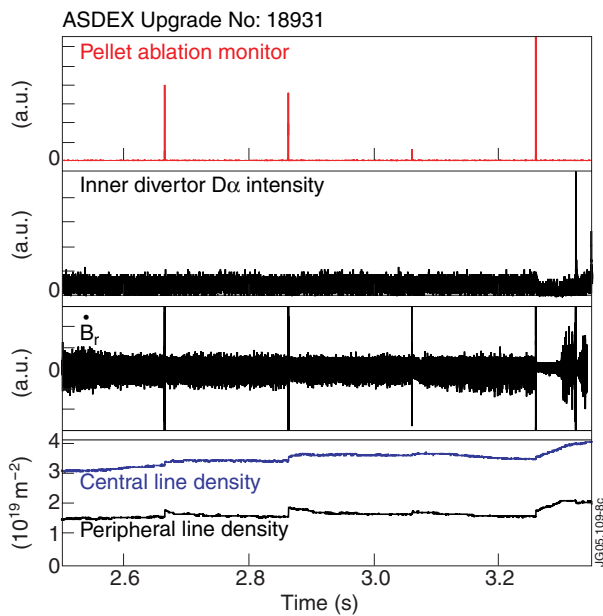


Figure 5: Injection of a train of pellets into QH-mode: After the fourth pellet (3.26s) the EHO vanishes and the density begins to rise (a) as the EHO activity ceases (b).

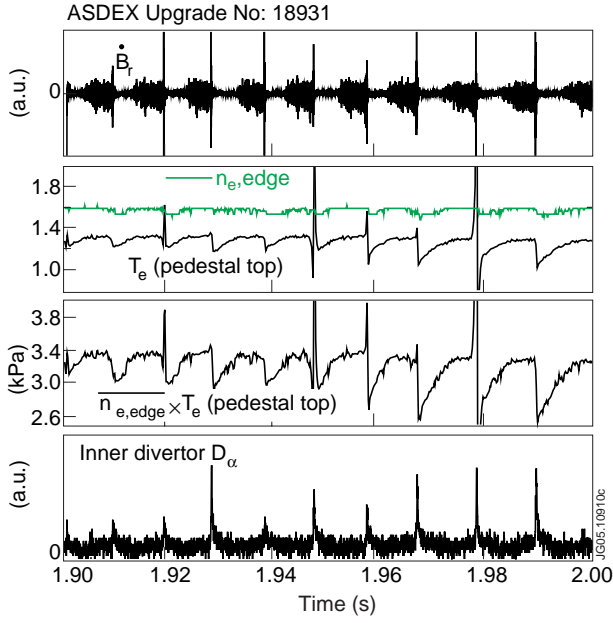


Figure 6: ELMy phase in a shot with counter-NBI. In between ELMs, the EHO appears as the pressure (approximated here as the product of edge line density and pedestal-top electron temperature) approaches its maximum. With EHO present, the pressure saturates.

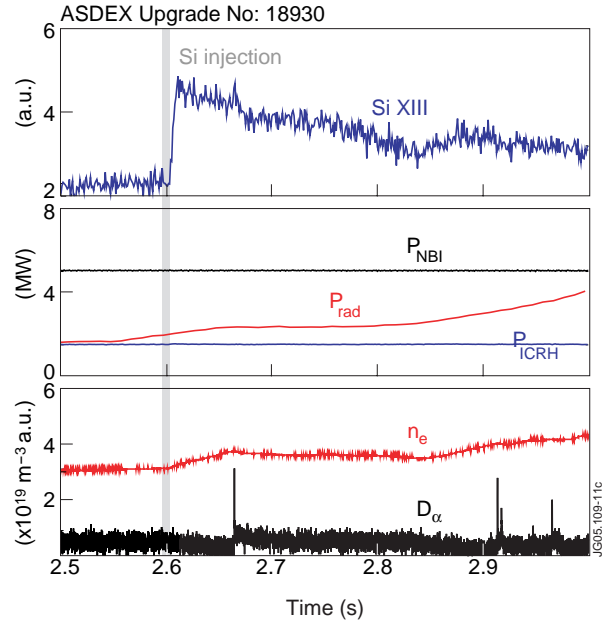


Figure 7: Impurity (Si) injection, monitored spectroscopically by Si XIII emission. The silicon content in the plasma continuously decreases after the injection.

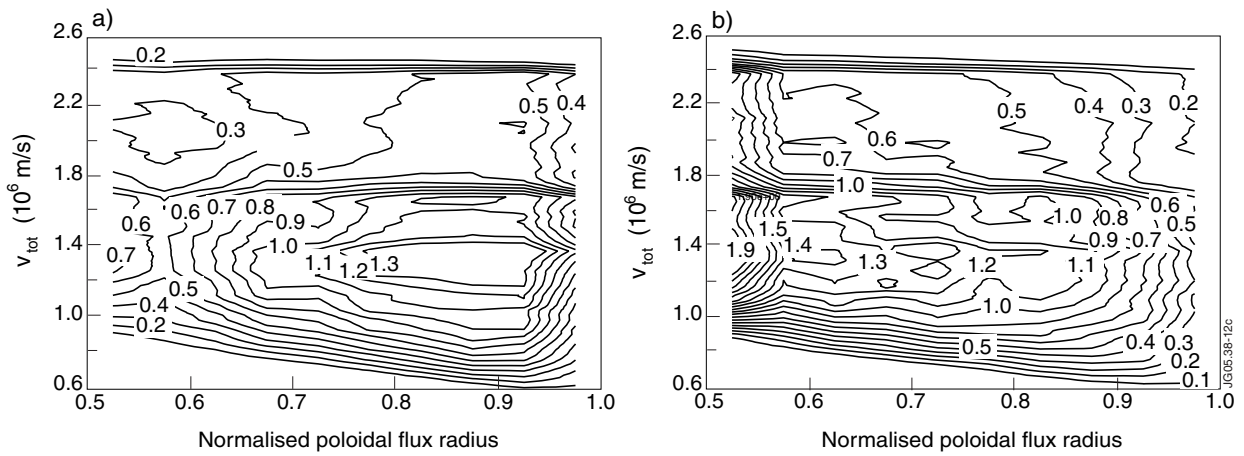


Figure 8: Fast particle distribution (a) for counter-injection as in AUG Pulse No: 17695 at  $t=5.6s$ , (b) for corresponding co-injection with identical background plasma.